ISSN 0001-4338, Izvestiya, Atmospheric and Oceanic Physics, 2022, Vol. 58, No. 3, pp. 302–313. © Pleiades Publishing, Ltd., 2022.
Russian Text © The Author(s), 2022, published in Izvestiya Rossiiskoi Akademii Nauk, Fizika Atmosfery i Okeana, 2022, Vol. 58, No. 3, pp. 352–364.

# Application of a Continuous Wavelet Transform to Study Planetary Waves[1]

**K. A. Didenko[a, b, *] and A. I. Pogoreltsev[a, b, †]**

[a] *Russian State Hydrometeorological University, St. Petersburg, 192007 Russia*
[b] *St. Petersburg State University, St. Petersburg-Petrodvorets, 198504 Russia*
**e-mail: didenko.xeniya@yandex.ru*

Received January 9, 2022; revised February 4, 2022; accepted February 9, 2022

**Abstract**—In this paper, we show a method for using the continuous Morlet wavelet transform in studying the variability of atmospheric migrating and nonmigrating tides. This approach makes it possible to obtain the amplitudes and phases of individual tidal components with different zonal wave numbers and periods. The most suitable periods required for data recovery are shown. The calculated amplitudes and phases are used to analyze the nonlinear interactions between stationary planetary waves and atmospheric tides.

**Keywords:** planetary waves, atmospheric tides, wavelet transform, nonlinear interactions

**DOI:** 10.1134/S0001433822030057

## INTRODUCTION

The question of the propagation of planetary waves in the atmosphere still occupies a central place in works on atmospheric dynamics. This is due to the influence of such waves on the general circulation and temperature regime, as well as on the distribution of ozone and other chemicals. In addition, an increase in the amplitude of the planetary wave is often observed in the stratosphere in winter, which leads to strong nonlinear phenomena. One of these phenomena is the generation of secondary waves caused by a nonlinear wave-wave interaction. Such effects are most pronounced during sudden stratospheric warmings (SSWs)—strong thermodynamic phenomena in the winter polar stratosphere that affect the middle atmosphere and also cause significant changes in the troposphere, mesosphere, and lower thermosphere. The emergence of SSWs is associated with the propagation of planetary waves from the troposphere to the stratosphere and their further interaction with the zonal circulation. During a SSW, a strong winter westerly stratospheric circulation is often replaced by a weak easterly wind for several days [1, 2].

Papers [3, 4] present a method for analyzing nonlinear interactions of stationary planetary waves, based on the study of the variability of the perturbation of potential enstrophy (Ertel's potential vorticity squared). In addition to the interaction of stationary planetary waves with zonal wave numbers $m_p = 1$ and 2 (SPW1 and SPW2) between themselves, they interact with diurnal or semidiurnal migrating thermal tides ($m_t = 1$ and 2). The latter, in turn, are periodic fluctuations on a global scale, which are caused by the absorption of solar radiation by the atmosphere-surface system, ozone and water vapor, as well as latent heat as a result of tropical deep convection [5, 6]. As a result of these interactions, diurnal and semidiurnal nonmigrating thermal tides arise with $m = m_t \pm m_p$ [7, 8]. Also, it is necessary to analyze the interaction of tidal components with each other.

Despite the fact that many works have been devoted to the study of thermal atmospheric tides, questions about their seasonal and annual variability remain. There is still a need to improve the modeling of tides in numerical models [9]. The study of the generation and variability of various tidal components is important for understanding the dynamics of not only the middle, but also the upper atmosphere. Temperature and wind perturbations associated with tides become very large in the mesosphere, penetrate into the thermosphere and significantly affect its momentum balance and thermodynamic balance [10]. In addition, the generation of nonmigrating atmospheric tides leads to longitudinal differences in the diurnal variations of the vertical wind and affects the intensity of hydroxyl emission and the concentration of atomic oxygen [11–13].

To consider the nonlinear interactions of stationary planetary waves and tides and/or tidal components with each other, it is necessary to obtain the amplitudes and phases of individual tidal components. To

[1] This paper was prepared on the basis of an oral report presented at the All-Russian Conference "Intrinsic Radiation, Structure and Dynamics of the Middle and Upper Atmosphere" (Moscow, November 22–23, 2021).

[†] Deceased.

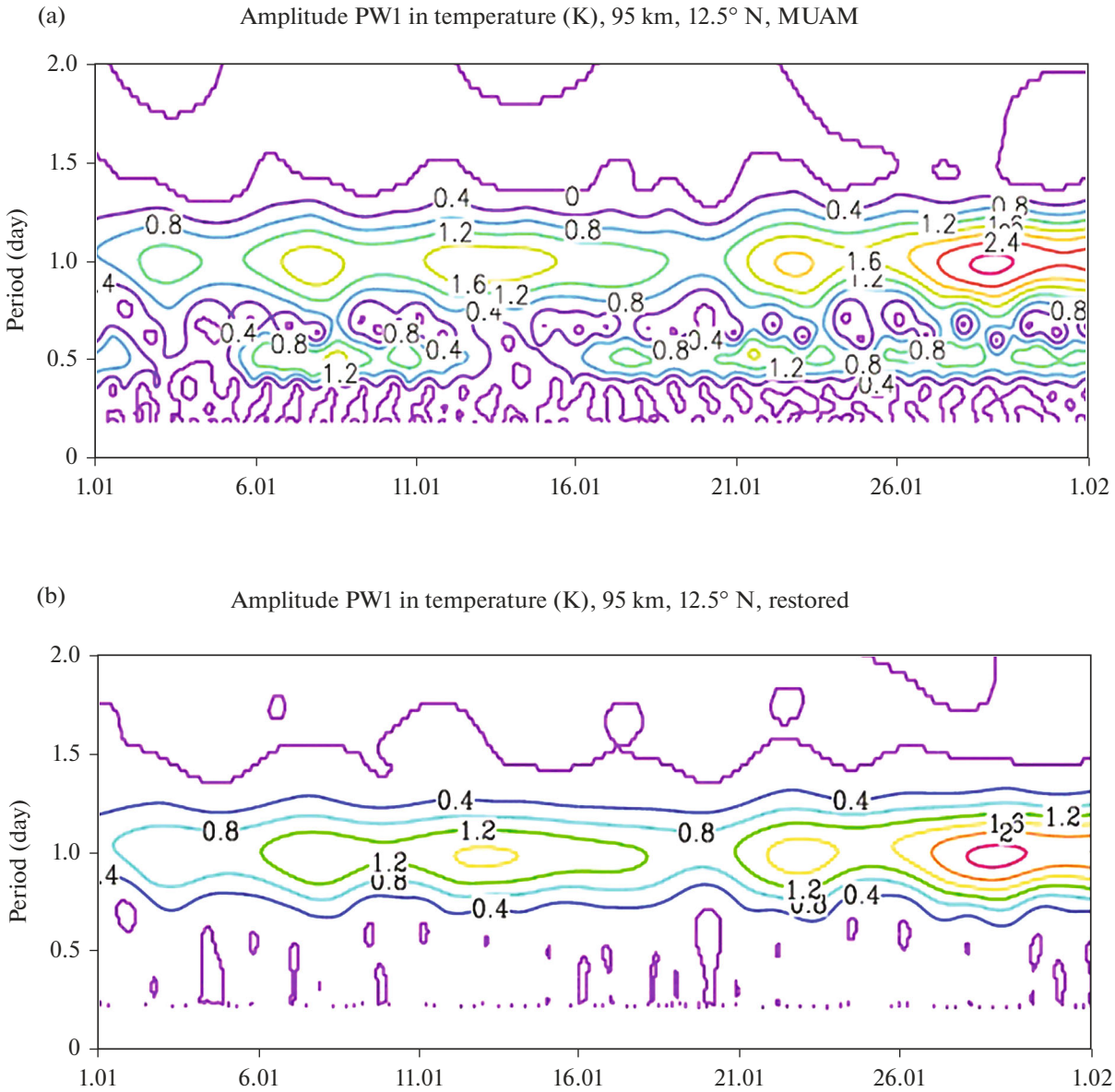


**Fig. 1.** Temporal variability of the amplitude of the planetary wave with $m = 1$ (PW1) at an altitude of 95 km, 12.5° N, January: (a) initial data; (b) data reconstructed after the wavelet transform for the interval of periods 0.7–1.25 (diurnal migrating tide).

do this, it was decided to use the results of calculations using the middle- and upper-atmosphere model (MUAM), a three-dimensional nonlinear model of the general circulation of the atmosphere from the surface to the heights of the F2 ionospheric layer, as initial data [7, 14]. Dimensionless log-isobaric height $x = -\ln(p/1000)$, where $p$ is the pressure in hPa, used as the vertical coordinate. The number of vertical levels can be arbitrary (from 48 to 60). The first version of the MUAM was developed based on the Cologne Model of the Middle Atmosphere–Leipzig Institute for Meteorology (COMMA_LIM) [15, 16]. In this work, we used a new version of the MUAM model, which includes parameterizations of atmospheric heating rates caused by latent heat release, which take into account both diurnal and longitudinal oscillations and the dependence on the El Niño–Southern Oscillation (ENSO) phase [17, 18]. An ensemble of solutions was obtained for the conditions of the El Niño neutral phase, the westerly phase of the quasi-biennial oscillation of the zonal wind in the equatorial stratosphere (QBO). For analysis, one of the members of the ensemble is selected, when the main sudden stratospheric warming was modeled in mid-January.

## 1. METHODOLOGY

The wavelet transform can be used to analyze time series containing nonstationary power at many differ-

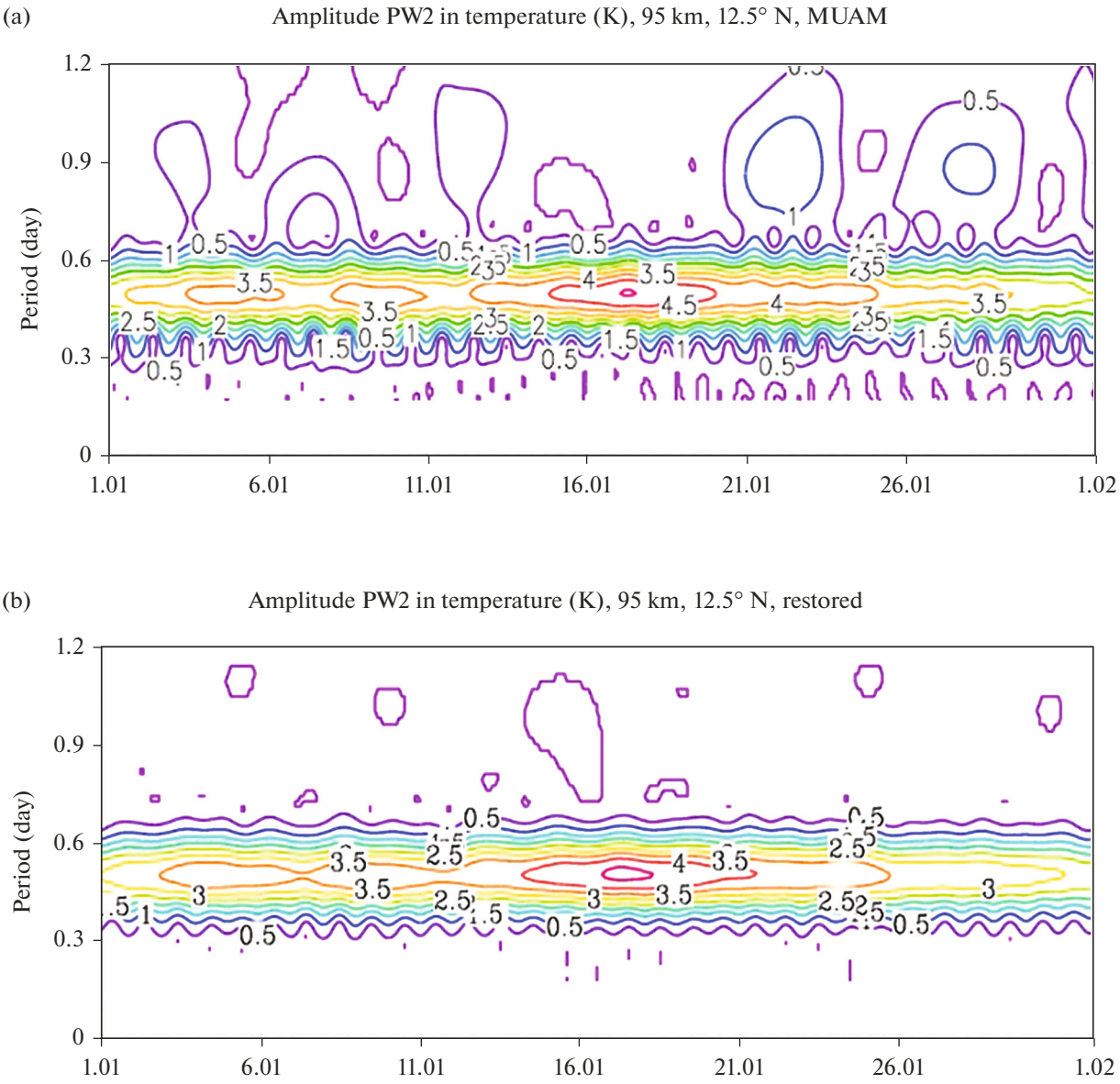


**Fig. 2.** Temporal variability of the amplitude of the planetary wave with $m = 2$ (PW2) at an altitude of 95 km, 12.5° N, January: (a) initial data; (b) data reconstructed after the wavelet transform for the interval of periods 0.25–0.7 (semidiurnal migrating tide).

ent frequencies, so it is often used in the study of both model and radar data. As a method for studying nonstationary signals, the Morlet wavelet transform is proposed. According to the model data, it was found that this wavelet transform is especially convenient for analyzing signals with a wide range of dominant frequencies localized in different time intervals, amplitude- and/or frequency-modulated spectral components, and singular wavelike phenomena that are observed in the neutral wind of the mesosphere/lower thermosphere and associated mainly with large-scale disturbances propagating from below [19, 20].

The model data contain fields of hydrodynamic quantities of the form $U(x, y, z, t)$ is the zonal wind, $V(x, y, z, t)$ is the meridional wind, and $T(x, y, z, t)$ is temperature. After Fourier expansion of these fields in longitude, we obtain time series of amplitudes and phases of individual zonal harmonics for all hydrodynamic quantities. In addition, using the complex Morlet wavelet transform, we obtain time series of amplitudes and phases of standing and east/west-propagating planetary waves, including atmospheric tides.

Since the wavelet transform is a bandpass filter with a known response function (wavelet function), it can be used to reconstruct the original time series, taking into account only certain harmonics. Time series restored after transformation $x_n(t)$ can be calculated using the following semi-empirical formula:

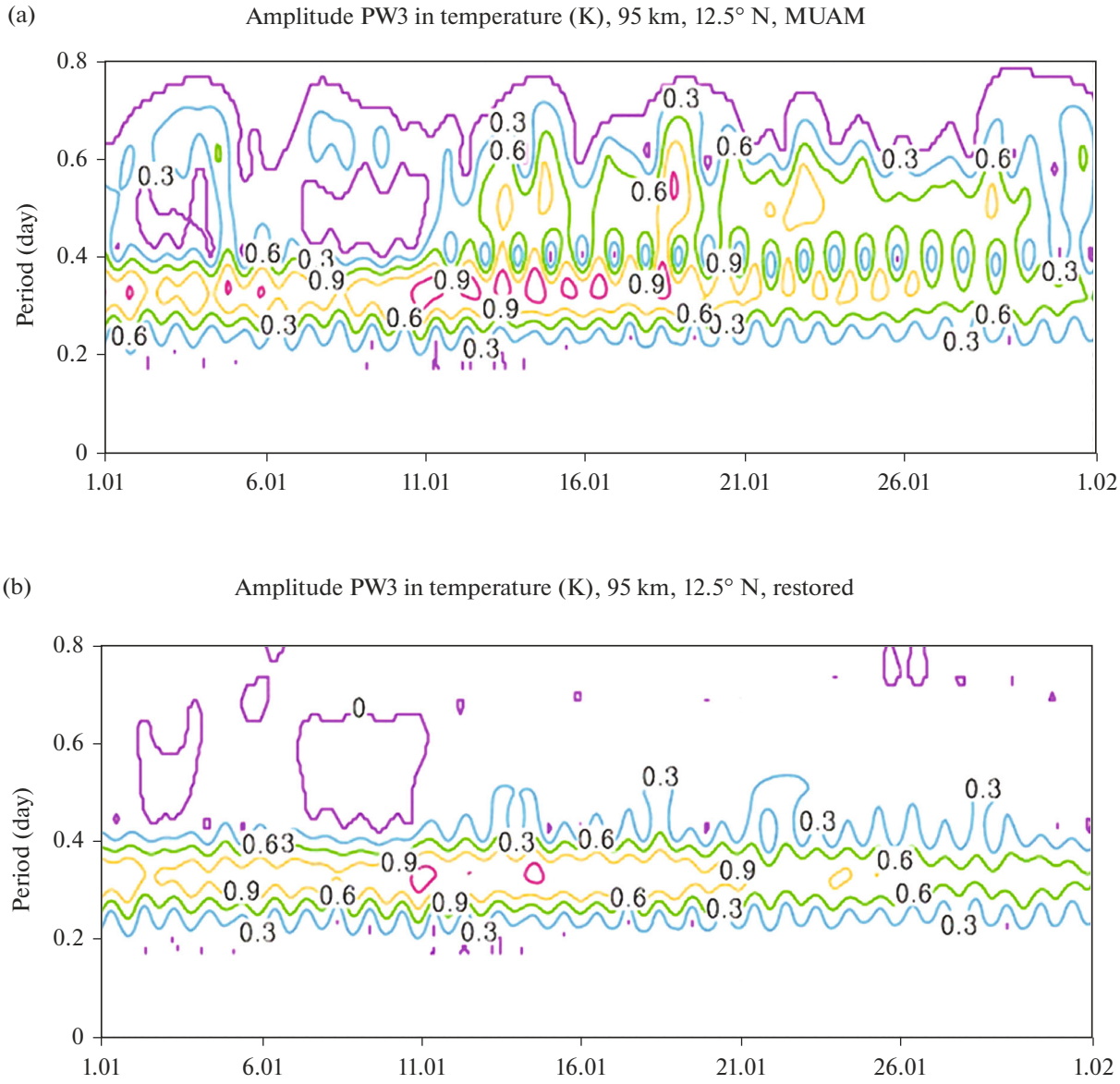


**Fig. 3.** Temporal variability of the amplitude of the planetary wave with $m = 3$ (PW3) at an altitude of 95 km, 12.5° N, January: (a) initial data; (b) data reconstructed after the wavelet transform for the interval of periods 0.15–0.45 (eight-hour migrating tide).

$$x_n(t) = \frac{\delta j \delta t^{1/2}}{C_\delta \psi_0(0)} \sum_{j=0}^{J} \frac{\mathrm{Re}\{W_n(s_j)\}}{s_j^{1/2}}, \qquad (1)$$

where summation is performed over all scales (periods), $J$ is the longest period, $\delta t$ is the reverse time interval, $\delta j$ is the scale interval, $\mathrm{Re}\{W_n(s_j)\}$ is the real part of the continuous wavelet power spectrum of the time series, and $s_j$ is the corresponding period.

Empirical coefficients with advisory values for the used Morlet wavelet—$C_\delta = 0{,}776$, $\delta j_0 = 0.6$, and $\psi_0(0) = \pi^{-1/4}$—transform the power spectrum into an amplitude spectrum and take into account energy scaling [21].

## 2. RESULTS OF APPLYING THE WAVELET TRANSFORM TO OBTAIN TIME SERIES OF AMPLITUDES AND PHASES OF INDIVIDUAL TIDAL HARMONICS

Using expression (1) and MUAM data, the fields of temperature, zonal, meridional wind, vertical velocity, and perturbations of the Ertel's potential vorticity were reconstructed. Figures 1–3 show as an example the temporal variability of the amplitude spectra of the atmospheric tide temperature field at 12.5° N. The results make it possible to determine data recovery periods not only for migrating tides, but also for nonmigrating tides. Later, the generation of tidal components can be analyzed separately using the filtered amplitudes and phases. In Figs. 1a and 3a, nonmigrat-

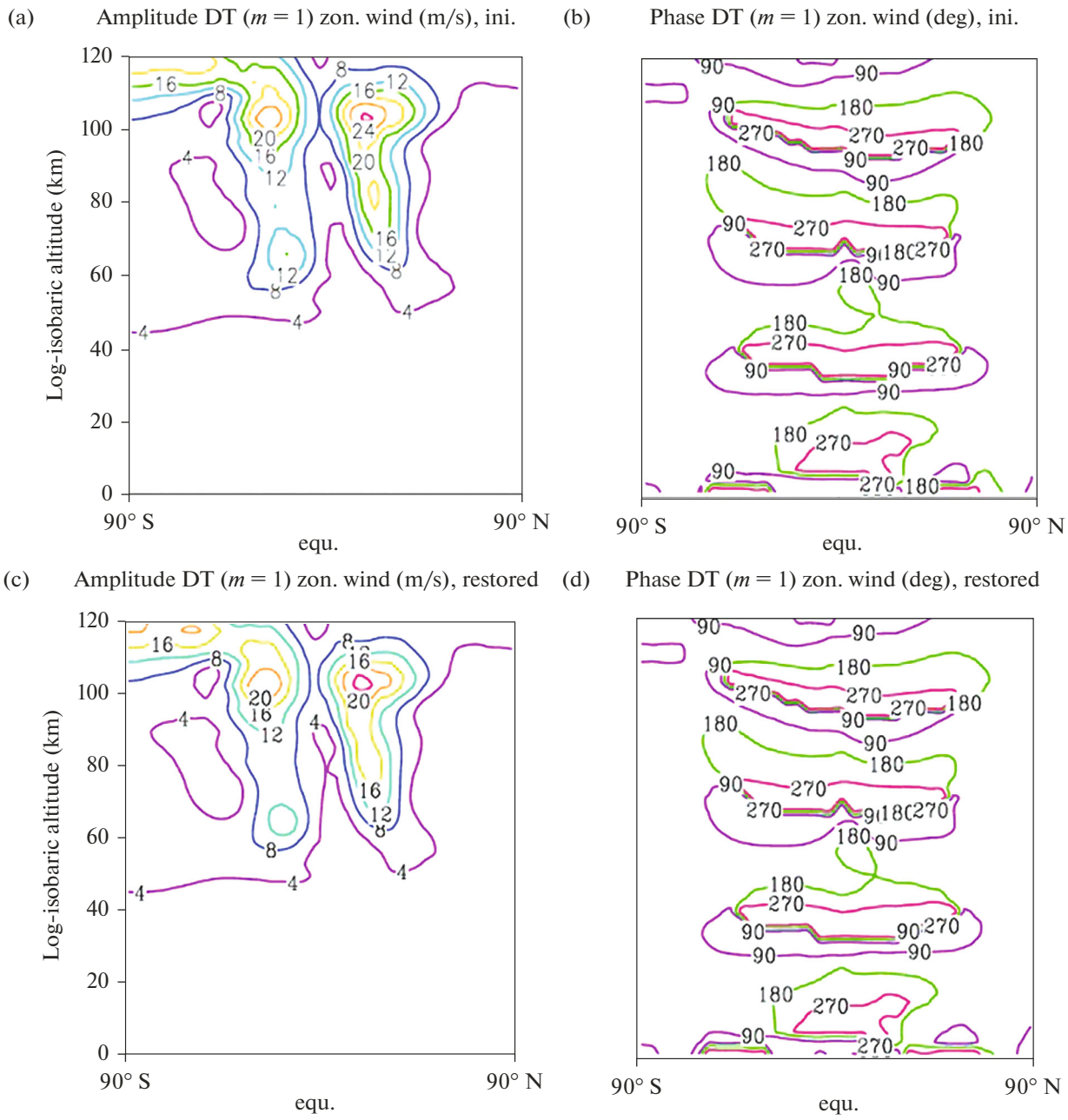


**Fig. 4.** Latitudinal-altitude distributions of the amplitude and phase of the diurnal tide in a zonal wind field: (a) amplitude, initial data; (b) phase, initial data; (c) amplitude, reconstructed data; and (d) phase, reconstructed data.

ing tides with $m = 1$ and 3, respectively, are observed with a period of 12 h. To restore the amplitudes of these tides, it is necessary to set periods of 0.3–0.7. In Fig. 2a, a nonmigrating tide is observed with a period of 24 h and $m = 2$, for restoring the amplitudes of which it is necessary to set periods of 0.7–1.2, as well as a nonmigrating tide with $m = 2$ and a period of 8 h. To restore it, it is necessary to select periods of 0.2–0.45. A nonmigrating tide with $m = 1$ and a period of 8 h is not observed.

Using the initial and reconstructed fields of temperature, zonal, meridional wind, vertical velocity, and perturbations of the potential Ertel's vorticity, one can also construct latitude-altitude distributions of amplitudes and phases for atmospheric tides. Figures 4–6 present the results for January for the zonal wind field of migrating tides, and Figs. 7–8 present those for nonmigrating ones.

The fields of temperature, zonal, meridional wind, vertical velocity, and perturbation of the potential Ertel's vorticity reconstructed using the complex Morlet wavelet transform were used in the study of nonlinear interactions between individual tidal components.

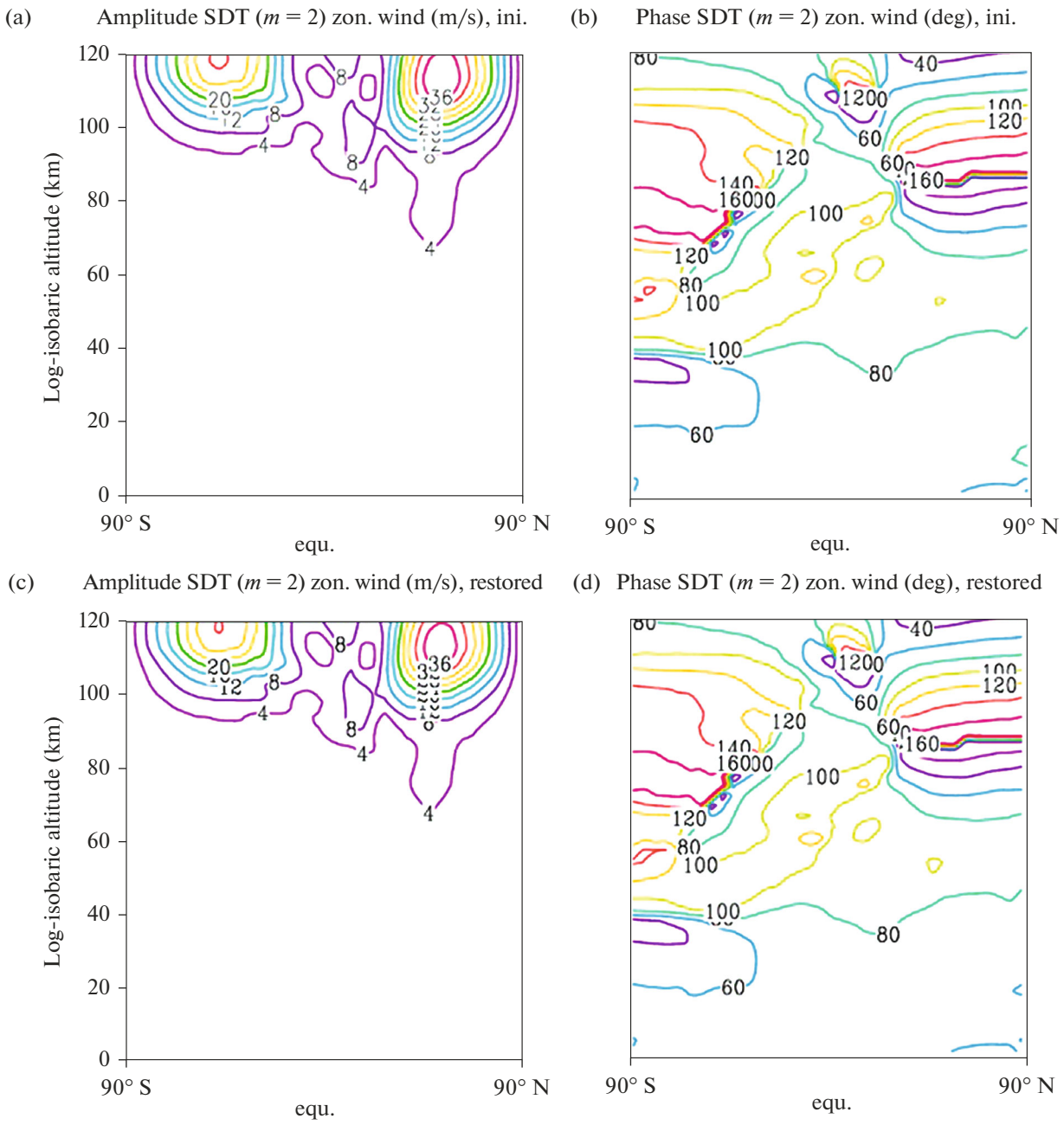


**Fig. 5.** Latitudinal-altitude distributions of the amplitude and phase of the semidiurnal tide in a zonal wind field: (a) amplitude, initial data; (b) phase, initial data; (c) amplitude, reconstructed data; and (d) phase, reconstructed data.

## 5. NONLINEAR INTERACTIONS

The method for analyzing nonlinear interactions of planetary waves, including solar thermal tides, is based on the study of the conservation of perturbed potential enstrophy. In this case, the terms responsible for the nonlinear interactions in the potential enstrophy balance equation are calculated. To obtain the balance equation, the Ertel's potential vorticity conservation equation is multiplied by its perturbation. General view of the balance of perturbed potential enstrophy in the log-isobaric coordinate system:

$$\frac{\partial}{\partial t}\left(\overline{P'^2}/2\right) = -\overline{P'(\vec{V}'\cdot\vec{\nabla}P')} - \overline{P'(\vec{V}'\cdot\vec{\nabla}\bar{P})} - \overline{P'(\bar{\vec{V}}\cdot\vec{\nabla}P')} + \overline{P'Q'}, \quad (2)$$

where $P$ is the potential Ertel's vorticity, which is equal to the scalar product of the absolute vorticity and the

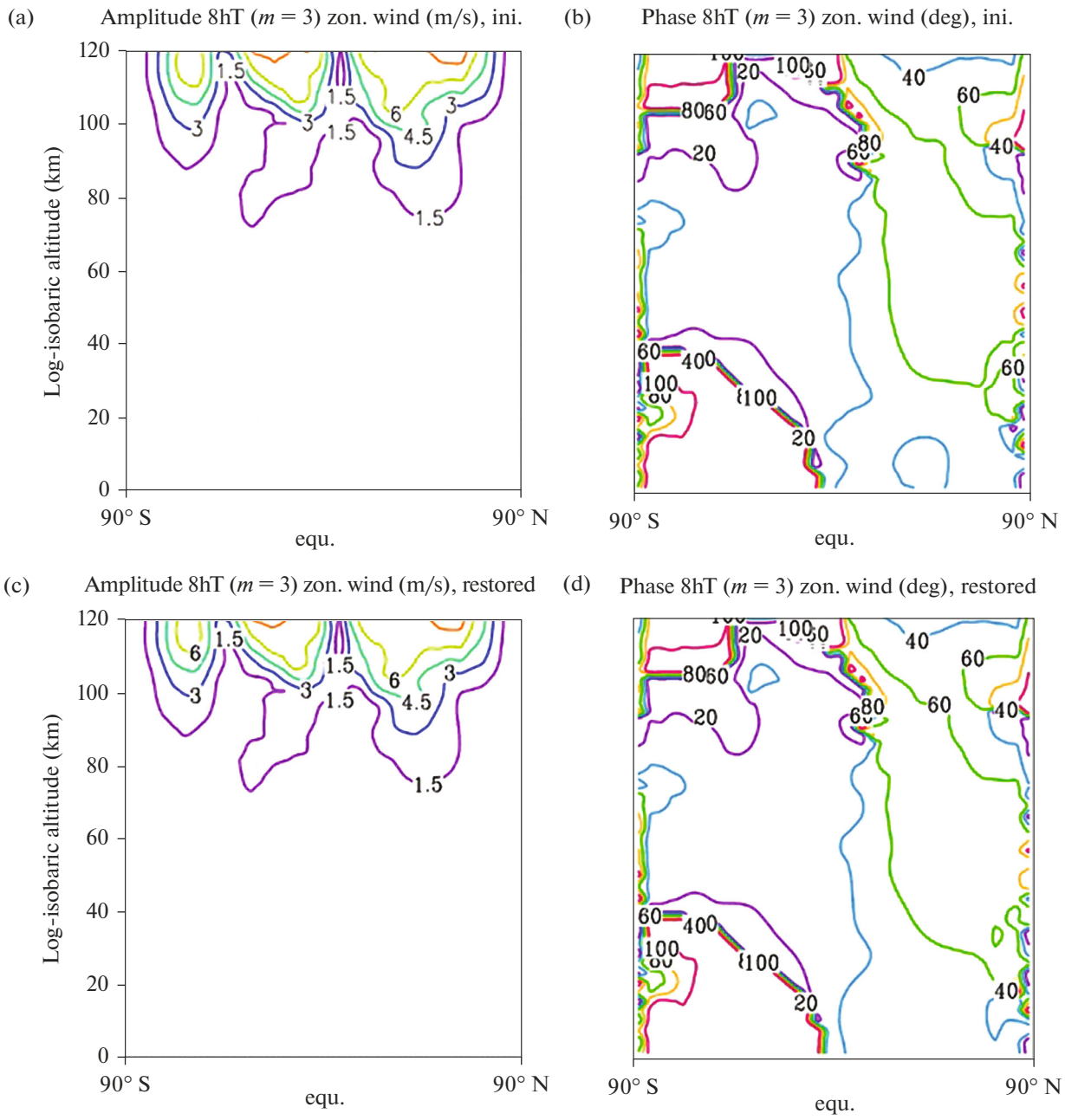


**Fig. 6.** Latitudinal-altitude distributions of amplitude and phase of 8-h tide in a zonal wind field: (a) amplitude, initial data; (b) phase, initial data; (c) amplitude, reconstructed data; and (d) phase, reconstructed data.

potential temperature gradient divided by the background density; $\vec{V}$ is the wind speed vector; and $Q'$ is the contribution of nonadiabatic heat inflows and/or dissipative terms. The overline means zonal averaging, and the dashes mean perturbations, i.e., deviations from zonal averaged values. The term on the left side of the equation is defined as a measure of the temporal variability of wave activity [22]. The first and second terms on the right side describe interactions of the wave–wave and wave-mean flow types, respectively. The next term is responsible for the advective transport of potential enstrophy. The latter on the right side describes the changes in perturbed potential enstrophy due to diabatic heating. This term also includes contributions to the momentum equation from gravitational and inertial–gravitational waves.

Taking into account the method of generation of secondary planetary waves shown in [3, 23], equations similar to Eq. (2) can be written for diurnal and semid-

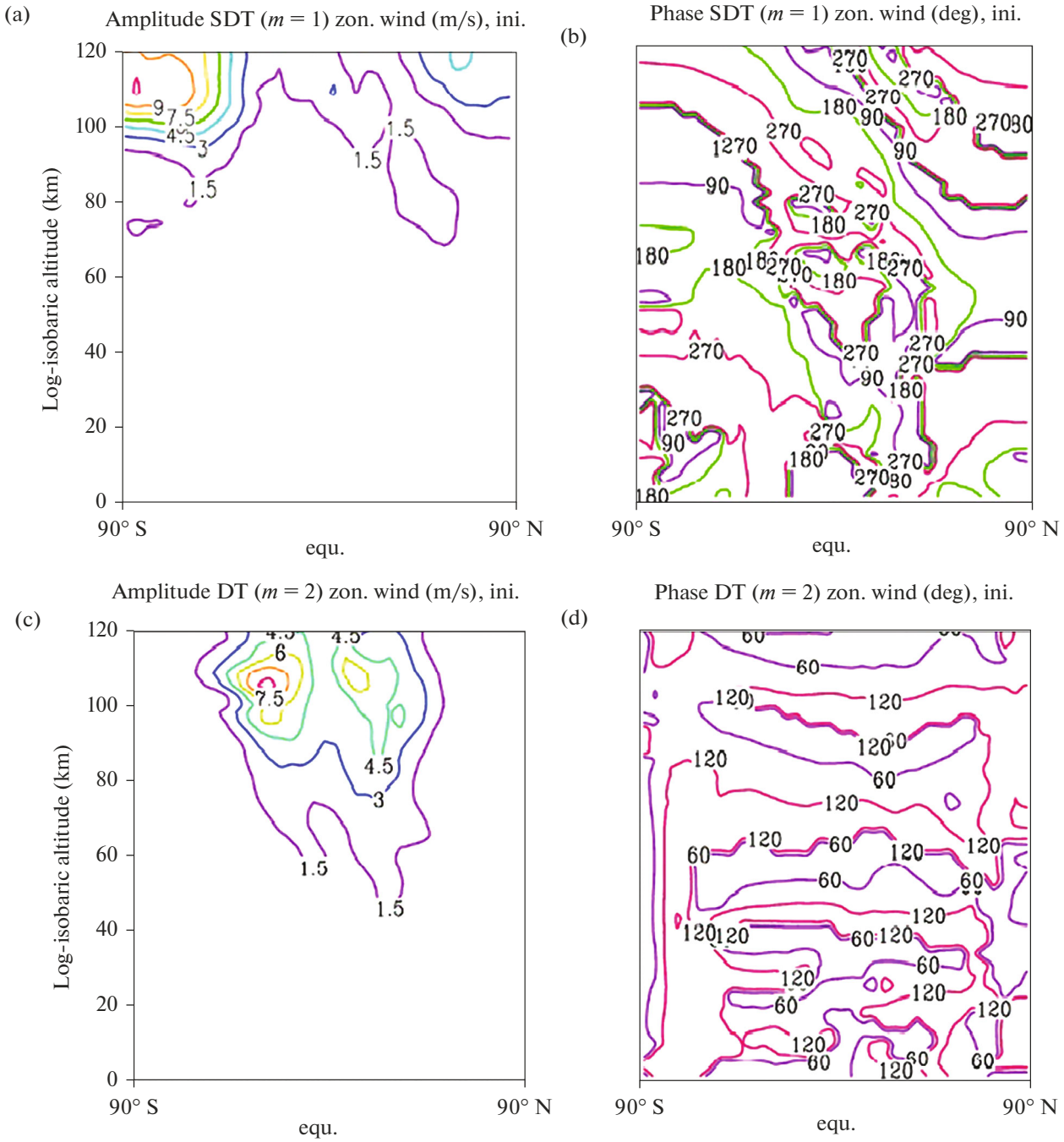


**Fig. 7.** Latitudinal-altitude distributions of the (a) amplitude and (b) phase of the semidiurnal nonmigrating tide and (c) amplitude and (d) phase of the diurnal nonmigrating tide in a field of the zonal wind.

iurnal migrating tides. According to this method, a diurnal migrating tide with $m_t = 1$ (DT) is generated as a result of the nonlinear interaction of the semidiurnal migrating tide (SDT, $m_t = 2$), as well as an 8-h migratory tide (8-h tide, $m_t = 3$) with an SDT; a semidiurnal migrating tide is generated as a result of the self-interaction of the DT and the interaction of an 8-h and DT tide. As a result, the balance equation of the disturbed potential enstrophy for diurnal and semidiurnal migrating tides, where the subscripts denote the zonal wave number, are Eqs. (3) and (4), respectively:

$$\frac{1}{2}\frac{\partial \overline{P_1'^2}}{\partial t} = -\overline{P_1'\left(\vec{V}_1' \cdot \vec{\nabla} P_2'\right)} - \overline{P_1'\left(\vec{V}_2' \cdot \vec{\nabla} P_1'\right)} - \overline{P_1'\left(\vec{V}_2' \cdot \vec{\nabla} P_3'\right)} - \overline{P_1'\left(\vec{V}_3' \cdot \vec{\nabla} P_2'\right)} - \overline{P_1'\left(\vec{V}_1' \cdot \vec{\nabla} \bar{P}\right)} - \overline{P_1'\left(\bar{\vec{V}} \cdot \vec{\nabla} P_1'\right)} + \overline{P_1' R_1'}, \quad (3)$$

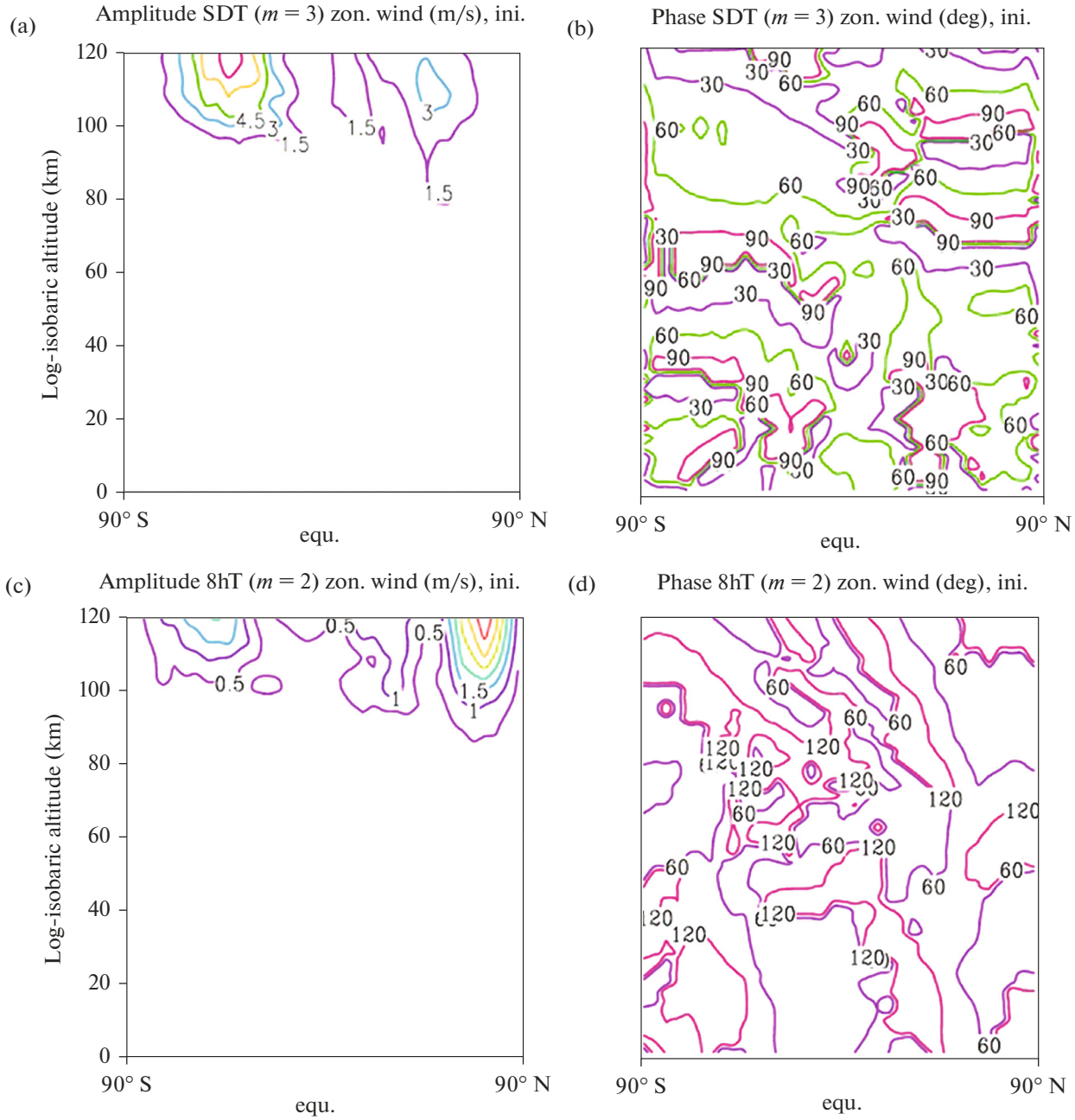


**Fig. 8.** Latitudinal-altitude distributions of the (a) amplitude and (b) phase of the semidiurnal nonmigrating tide and (c) amplitudes and (d) phase of an 8-h nonmigrating tide in a the zonal wind field.

$$\frac{1}{2}\frac{\partial \overline{P_2'^2}}{\partial t} = -\overline{P_2'\left(\vec{V}_1' \cdot \vec{\nabla} P_1'\right)} - \overline{P_2'\left(\vec{V}_1' \cdot \vec{\nabla} P_3'\right)} - \overline{P_2'\left(\vec{V}_3' \cdot \vec{\nabla} P_1'\right)} - \overline{P_2'\left(\vec{V}_2' \cdot \vec{\nabla} \bar{P}\right)} - \overline{P_2'\left(\bar{\vec{V}} \cdot \vec{\nabla} P_2'\right)} + \overline{P_2' R_2'}. \quad (4)$$

The amplitudes and phases of the tidal components obtained by the method described in Section 2 were used to analyze the nonlinear interactions between migrating atmospheric tides and the mean flow, as well as between themselves. Figures 9–10 show the results of calculating the terms in Eqs. (3) and (4) for 95 km averaged over the latitude band 52.5°–62.5° N with a scale cosine of latitude. Panels (a) show the temporal variability of wave activity, panels (b) and (c) show the interaction between migrating tides, and panel (d) shows the interaction between the tide and the mean flow. The values along the *y* axis are given in units of $10^{12}$(kg m$^{-3}$)$^2$ *PVU*$^2$/day, where 1 *PVU* (potential vorticity unit) = $10^{-6}$ K m$^2$ kg$^{-1}$ s$^{-1}$.

The calculation results show that, at an altitude of 95 km, the contribution of the terms responsible for the nonlinear interaction between tides is comparable

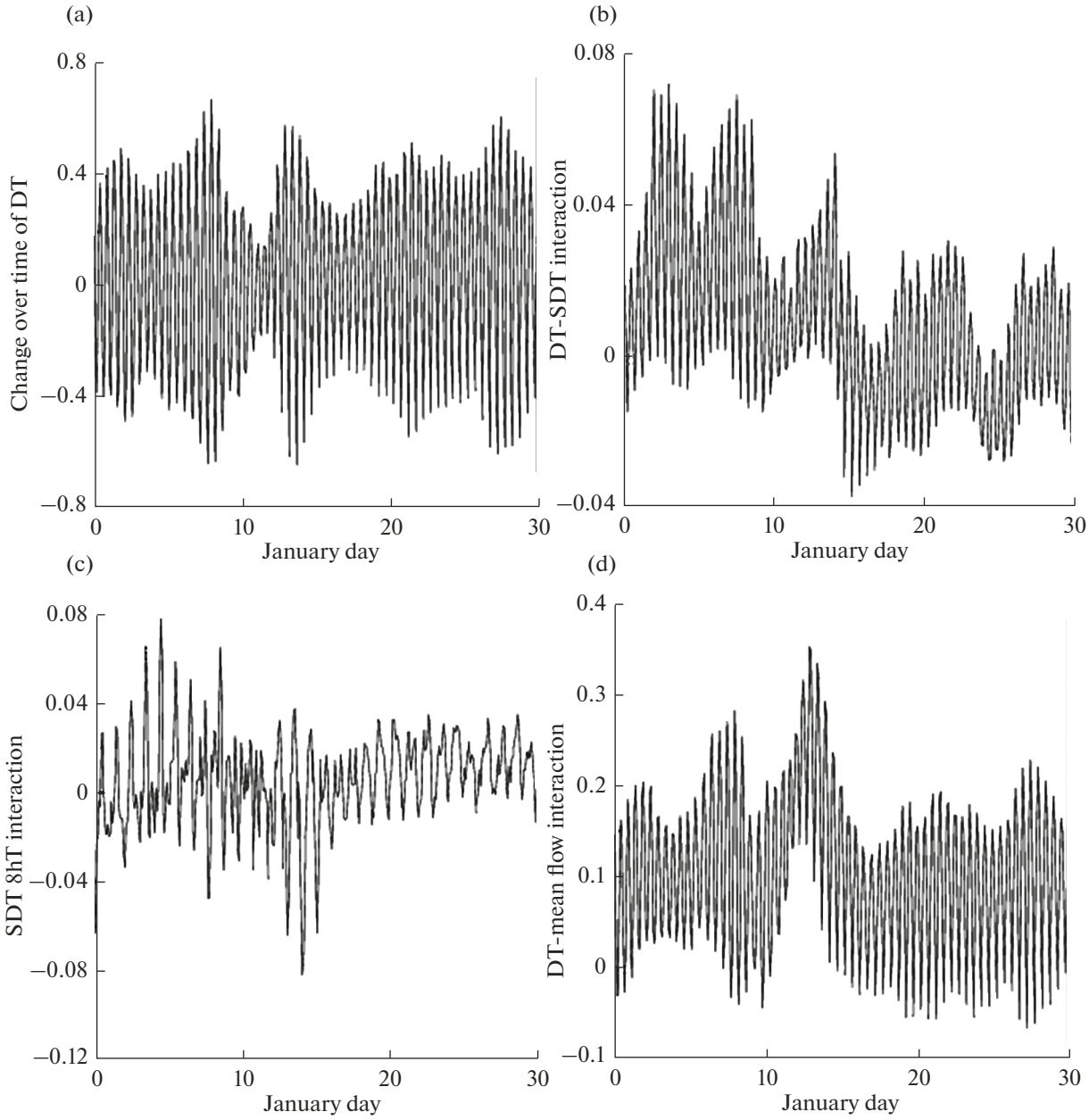


**Fig. 9.** Terms responsible for the contribution to the balance equation of the disturbed potential enstrophy for the diurnal migrating tide, MUAM, January.

with the contribution of the other terms. Thus, model data available up to ionospheric heights have an advantage over reanalysis data in tidal studies. The results are affected by the strong variability of atmospheric tides, especially diurnal ones. A decrease in the wave activity of the diurnal tide is accompanied by an increase in the semidiurnal tide (Figs. 9a and 10a), and changes are observed during the development of a sudden stratospheric warming. Similar results were obtained when analyzing the interaction of a wave with an average flow (Figs. 9d, 10d). The calculation of wave-wave interactions shows a significant contribution of the 8-h tide to the generation of atmospheric tides. It should be noted that the generation of the diurnal tide is intense before the onset of stratospheric warming and the generation of the semidiurnal tide is intense during its development.

## 6. CONCLUSIONS

The results of numerical simulation are used to study the nonlinear interaction of planetary waves and the variability of migrating and nonmigrating tides. A method is presented that makes it possible to obtain

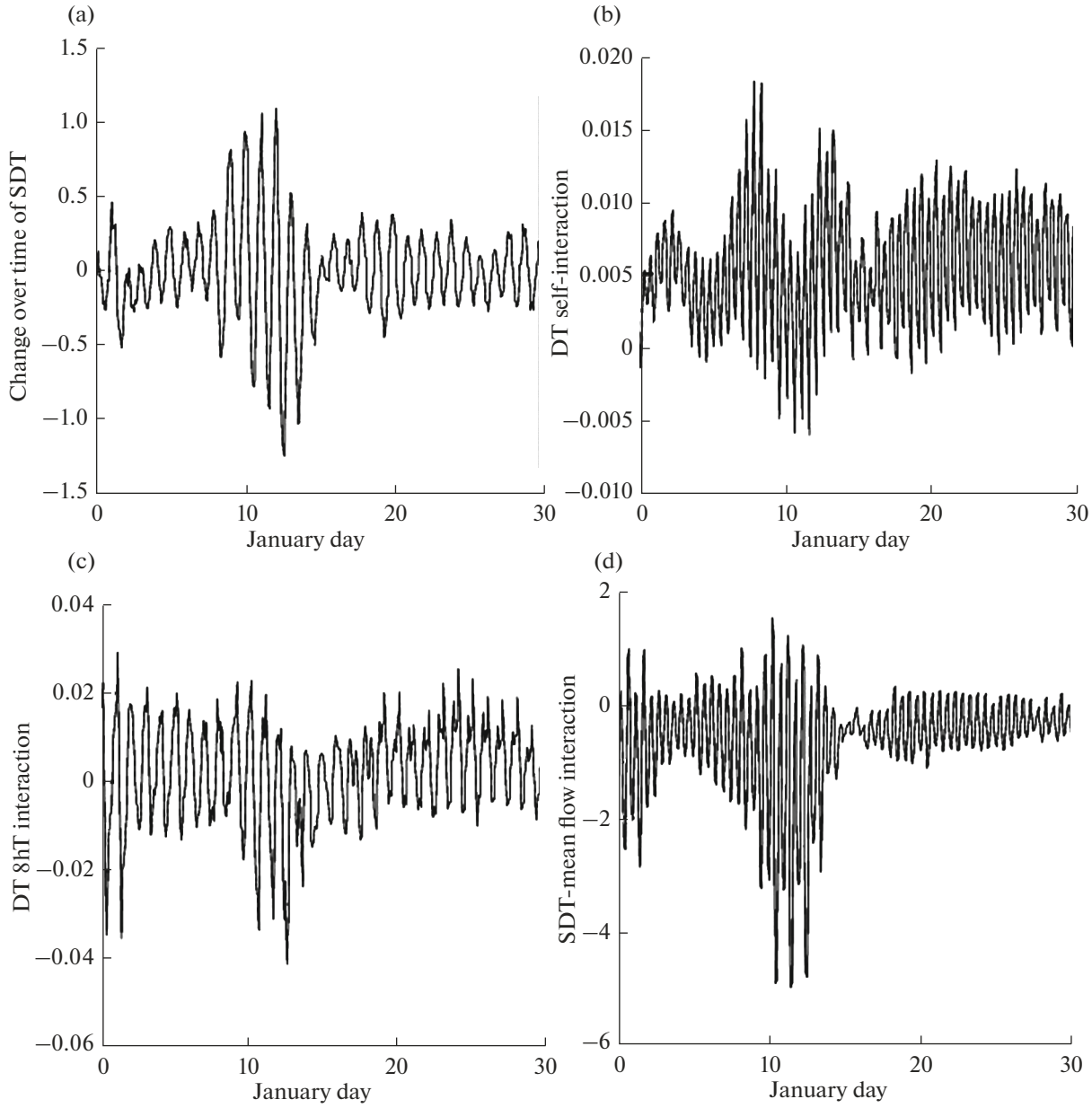


**Fig. 10.** Terms responsible for the contribution to the equation of balance of the disturbed potential enstrophy for the semidiurnal migrating tide, MUAM, January.

the amplitudes and phases of individual tidal components with different zonal wave numbers and periods. The results show that the complex Morlet wavelet transform can be used to reconstruct not only radar data, but also model data, and the fields of the wind speed, temperature, and potential Ertel vorticity components are perfectly restored at specified intervals of periods. The necessary periods for the recovery of nonmigrating tides were determined. It can also be noted that the maximum amplitudes of nonmigrating tides (except for the 8-h $m = 2$) are observed at the levels of the upper atmosphere, mainly in the Southern Hemisphere.

The obtained amplitudes and phases were used to calculate the terms in the balance of the perturbed potential enstrophy, which describe the nonlinear interactions between planetary waves. The contribution of the terms responsible for the variability of wave activity in time, the interaction between waves, and the interaction of a wave with an average flow is shown. At the levels of the mesosphere/lower thermosphere, the contribution of various terms to the equation of perturbed potential enstrophy is comparable. The contribution of the 8-h migrating tide to the generation of wave motions is noted. In addition, dynamic phenomena in the stratosphere, such as sudden strato-

spheric warmings, are accompanied by a decrease in the wave activity of the diurnal tide and an increase in the semidiurnal one. This approach and the obtained amplitudes and phases can be used in the study of the generation of nonmigrating atmospheric thermal tides. This will be the subject of further research.

## FUNDING

This work was carried out with the financial support of the Russian Science Foundation within the framework of scientific project no. 20-77-10006.

## CONFLICT OF INTEREST

The authors declare that they have no conflicts of interest.

## REFERENCES

1. M. Baldwin, B. Ayarzaguena, T. Birner, N. Butchart, A. Butler, A. Charlton-Perez, D. Domeisen, C. Garfinkel, H. Garny, E. Gerber, M. Hegglin, U. Langematz, and N. Pedatella, "Sudden stratospheric warmings," Rev. Geophys. **58**, 1–37 (2021).
2. P. N. Vargin, E. M. Volodin, A. Yu. Karpechko, and A. I. Pogoreltsev, "Stratosphere–troposphere interactions," Herald Russ. Acad. Sci. **85** (1), 56–63 (2015).
3. K. A. Didenko, T. S. Ermakova, A. V. Koval', and A. I. Pogorel'tsev, "Diagnostics of nonlinear interactions of stationary planetary waves," Uch. Zap. RGGMU, No. 56, 19–29 (2019).
4. K. A. Didenko, A. I. Pogoreltsev, T. S. Ermakova, and G. M. Shved, "Nonlinear Interactions of stationary planetary waves during February 2016 sudden stratospheric warming," IOP Conf. Ser.: Earth Environ. Sci., No. 386, 1–7 (2019).
5. M. Baldwin, T. Birner, G. Brasseur, J. Burrows, N. Butchart, R. Garcia, M. Geller, L. Gray, K. Hamilton, N. Harnik, M. Hegglin, U. Langematz, A. Robock, K. Sato, and A. Scaife, "100 years of progress in understanding the stratosphere and mesosphere," Meteorol. Monogr. **59** (27), 27.1–27.61 (2019).
6. G. M. Shved, *Introduction to Atmospheric Dynamics and Energetics* (S.-Peterb. Univ., St. Petersburg, 2020) [In Russian].
7. A. I. Pogoreltsev, A. A. Vlasov, K. Fröhlich, and Ch. Jacobi, "Planetary waves in coupling the lower and upper atmosphere," J. Atmos. Sol.-Terr. Phys. **69**, 2083–2101 (2007).
8. E. V. Suvorova and A. I. Pogoreltsev, "Modeling of nonmigrating tides in the middle atmosphere," Geomagn. Aeron. (Engl. Transl.) **51** (1), 105–115 (2011).
9. R. N. Davis, J. Du, A. K. Smith, W. E. Ward, and N. J. Mitchell, "The diurnal and semidiurnal tides over Ascension Island (88° S, 148° W) and their interaction with the stratospheric quasibiennial oscillation: Studies with meteor radar, eCMAM and WACCM," Atmos. Chem. Phys. **13**, 9543–9564 (2013).
10. E. Becker, "Mean-flow effects of thermal tides in the mesosphere and lower thermosphere," J. Atmos. Sci. **74**, 2043–2063 (2017).
11. I. V. Medvedeva, A. I. Semenov, A. I. Pogoreltsev, and A. V. Tatarnikov, "Influence of sudden stratospheric warming on the mesosphere/lower thermosphere from the hydroxyl emission observations and numerical simulations," J. Atmos. Sol.-Terr. Phys. **187**, 22–32 (2019).
12. Y. I. Portnyagin, J. M. Forbes, N. A. Makarov, E. G. Merzlyakov, and S. Palo, "The summertime 12-h wind oscillation with zonal wavenumber $s = 1$ in the lower thermosphere over the South Pole," Ann. Geophys. **16**, 828 (1998).
13. S. M. Dempsey, N. P. Hindley, T. Moffat-Griffin, C. J. Wright, A. K. Smith, J. Du, and N. J. Mitchell, "Winds and tides of the Antarctic mesosphere and lower thermosphere: One year of meteor-radar observations over Rothera (68° S, 68° W) and comparisons with WACCM and eCMAM," J. Atmos. Sol.-Terr. Phys. **212**, 1 (2021).
14. K. Fröhlich, A. I. Pogoreltsev, and Ch. Jacobi, "Numerical simulation of tides, Rossby and Kelvin waves with the COMMA-LIM model," Adv. Space Res. **32**, 863–868 (2003).
15. K. Fröhlich, A. I. Pogoreltsev, and Ch. Jacobi, "The 48-layer COMMA-LIM model," Rep. Inst. Meteorol. Univ. Leipzig, No. 30, 157–185 (2003).
16. N. M. Gavrilov, A. I. Pogoreltsev, and Ch. Jacobi, "Numerical modeling of the effect of latitude-inhomogeneous gravity waves on the circulation of the middle atmosphere," Izv., Atmos. Ocean. Phys. **41** (1), 9–18 (2005).
17. A. I. Pogoreltsev, A. A. Vlasov, K. Fröhlich, and Ch. Jacobi, "Planetary waves in coupling the lower and upper atmosphere," J. Atmos. Sol.-Terr. Phys. **69**, 2083–2101 (2007).
18. T. S. Ermakova, O. G. Aniskina, I. A. Statnaia, M. A. Motsakov, and A. I. Pogoreltsev, "Simulation of the ENSO influence on the extra-tropical middle atmosphere," Earth Planets Space **71** (8), 1–9 (2019).
19. D. Pancheva, A. G. Beard, and N. J. Mitchell, "Nonlinear interactions between planetary waves in the mesosphere/lower-thermosphere region," J. Geophys. Res. **105** (A1), 157–170 (2000).
20. C. Chen and X. Chu, "Two-dimensional Morlet wavelet transform and its application to wave recognition methodology of automatically extracting two-dimensional wave packets from lidar observations in Antarctica," J. Atmos. Sol.-Terr. Phys. **162**, 28–47 (2017).
21. C. Torrence and P. G. Compo, "A practical guide to wavelet analysis," Bull. Am. Meteorol. Soc. **79**, 65–67 (1998).
22. I. P. White, L. Hua, N. J. Mitchell, and T. Phillips, "Dynamical response to the QBO in the Northern winter stratosphere: signatures in wave forcing and eddy fluxes of potential vorticity," J. Atmos. Sci. **72**, 4487–4507 (2015).
23. A. I. Pogoreltsev, "Numerical simulation of secondary planetary waves arising from the nonlinear interaction of the normal atmospheric modes," Phys. Chem. Earth (Part C) **26** (6), 395–403 (2001).